Reprinted from ENGINEERING FOR POWER, *Vol. 102, No. 1, January 1980*

A. Ray[1]
D. A. Berkowitz[2]
V. H. Sumaria
The MITRE Corporation, Bedford, Mass.

Nonlinear Dynamic Model of a Fluidized-Bed Steam Generation System

A dynamic model of an atmospheric pressure fluidized-bed steam generation system is presented which allows digital simulation and analytical controller design. The nonlinear, time-invariant, deterministic, continuous-time model is derived in state-space form from conservation relations, empirical correlations and system design data. The model has been verified for steady-state and transient performance with measured data from experimental test runs. Transient responses of several process variables, following independent step disturbances in coal feed rate and air flow, are illustrated.

Introduction

Fluidized-bed combustion (FBC) is an alternative technique being considered for application to commercial scale electric power generation. Fluidized-bed technology is well known in chemical engineering and fuel processing industries [1]. For coal combustion, the fluidized bed furnace offers an alternative to scrubbers for capturing flue gas SO_2.

Several fluidized-bed combustion facilities with equivalent capacities in the range 1–10 MWe are in operation at present, or in various stages of design and construction [2]. A 30 MWe multicell unit installed at Monongahela Power Company's Rivesville Station in West Virginia is now being tested. 200 MWe plants suitable for commercial use by utility companies are being considered. This technology is being developed much more rapidly than has been the case with conventional fossil power plants. Mathematical modeling and simulation are useful tools for analyzing performance and control problems in complex, interactive systems such as power plants [3, 4]; their application to FBC systems is very timely.

This paper presents a nonlinear dynamic model of an atmospheric pressure FBC steam generation system, which allows digital simulation and analytical controller design. The model provides the basis for: (1) understanding complex and interactive process dynamics, (2) design verification and predicting effects of subsystem changes on the entire process, (3) interactive multivariable controller design, and (4) overall system (process and controller) performance evaluation. The model was verified with experimental measurements for both steady-state and transient performance. Although related to a particular system, the modeling and simulation techniques presented in this paper have general applicability and can be readily adapted to other fluidized-bed power generation systems.

Model equations are solved numerically using CSMP-III [5]. A FORTRAN version of the CSMP-III code is incorporated as a subroutine in general purpose analytical programs to obtain steady-state solutions, for model linearization, and for other purposes such as eigenvalue and transfer function determination [6].

System Description

In fluidized-bed combustion, coal particles of about 1 cm top size are introduced pneumatically into a course bed of calcined limestone. The major bed particle dimension is about 3 mm. At any instant, coal fraction in the bed is about 2 percent; once coal has ignited, combustion is self-sustaining. Coal separates into a volatile component and a solid component of char and ash. A portion of the char and ash are blown out of the bed, or elutriated, with the flue gas.

Calcined limestone, CaO, acts as SO_2 sorbent. It reacts with O_2 and SO_2 in the bed to form $CaSO_4$. As the amount of available limestone decreases, it is necessary to add fresh limestone with the coal. With continual addition of fresh bed material, spent bed material must be removed to maintain constant bed mass or bed height. In addition, continual bed recirculation and screening removes nonreactive bed material.

To optimize sorbent effectiveness, and to avoid ash sticking and agglomerating, fluidized-bed temperature is controlled to approximately 840°C (1550°F) Thermal energy is continually removed from the bed by water or steam cooled heat transfer surface. Use of immersed heat transfer assemblies gives the fluidized-bed boiler its major distinctive feature, creating at the same time several advantages and several new problems.

Above the minimum fluidization condition, pressure drop across the bed varies very little with further increases in superficial air velocity, and remains equal to weight per unit area of the bed. The air distributor plate and bed geometry are designed to minimize occurrence of channeling and unstable flow which alter the fluidization characteristic.

Combustion occurs primarily within the bed (overbed combustion accounts for a small portion of the energy release), and bed heat transfer is a combination of conduction, convection and radiation. Heat transfer rate to immersed surfaces is high, but only weakly dependent on fluidizing air velocity in the normal operating range [1].

Contributed by the Power Division of THE AMERICAN SOCIETY OF MECHANICAL ENGINEERING for publication in the JOURNAL OF ENGINEERING FOR POWER. Manuscript received at ASME Headquarters October 18, 1978.

[1] Currently Assistant Professor of Mechanical Engineering, Carnegie-Mellon University, Pittsburgh, PA 15213.

[2] Currently with JAYCOR, Bedford, MA 01730.

The atmospheric pressure fluidized-bed Process Development Unit (PDU) at Alexandria, Virginia, has a single cell 1.83 m × 0.46 m (6 ft × 1.5 ft) with steam generating capacity of 0.63 kg/s (5000 lbm/hr) at 1.724×10^6 N/m^2 (250 psia) and 204°C (400°F), equivalent to approximately 0.5 MWe. The schematic in Fig. 1 includes major components that were modeled. The immersed cooling water bundle was removed during the particular experiments reported here, and was removed from the model, as well. Waterwalls were the only immersed heat transfer surfaces in the bed.

Modeling Approach

The physical process consists of distributed parameter dynamic elements, most generally represented by nonlinear partial differential equations with space and time as independent variables. To obtain numerical solutions, the partial differential equations are approximated by a finite set of ordinary differential equations with time as the independent variable. This approach has proven to be adequate in the simulation of other power generation systems [7–9].

A model solution diagram for the fluidized-bed plant is shown in Fig. 2. Each block represents a physical component or group of components. Lines interconnecting blocks indicate direction of information flow or "model causality." This diagram shows how individual component models mathematically interface with each other, and ensures consistent causality for the complete set of equations defining the physical process.

Following the arrangement in Fig. 2, plant modeling is accomplished in two steps: (1) modeling of individual components or groups of components and (2) formulation of an overall plant model by appropriate interconnection of the individual component models.

Step 1 includes determination of steady-state solutions and eigenvalues (of linearized models) at several operating points. Steady-state solutions are verified with design data and eigenvalues are examined for frequency range. Step 2 incorporates sequential interconnection of component models according to the solution diagram. Steady-state solutions and eigenvalues of the augmented model are examined at each phase of interconnection.

Development of Model Equations

Model structure is formulated from: conservation relations for mass, momentum, and energy, semi-empirical relationships for fluid flow and heat transfer, and state relations for thermodynamic properties of working fluids. Model parameters are evaluated from design and experimental data.

Major assumptions in addition to the lumped parameter approximation are: (1) uniform fluid flow over pipe, duct or furnace cross-section, (2) perfect thermal insulation between plant components and

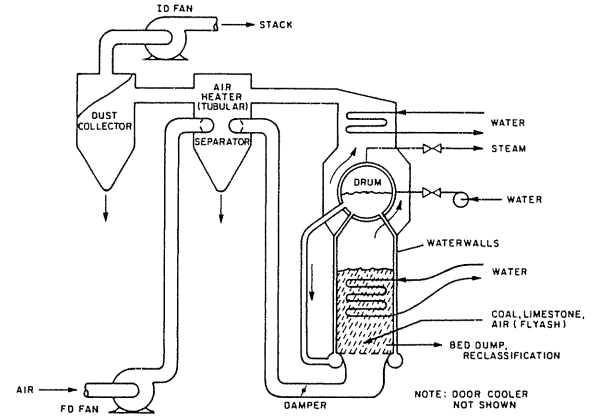

Fig. 1 Atmospheric Pressure fluidized-bed Process Development Unit (PDU), Alexandria, Va

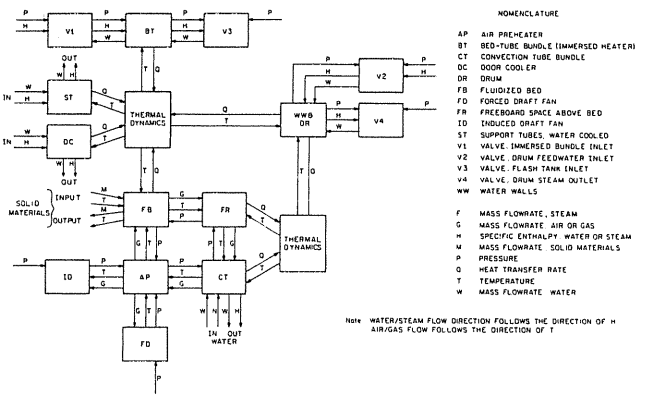

Fig. 2 Model solution diagram

the environment, (3) negligible pressure drop due to velocity and gravitational heads in gas and steam paths, (4) uniform fluidized-bed temperature, (5) coal division into solid and gas fractions independent of superficial air velocity, (7) constant average value of coal particle residence time in the fluidized bed, (8) elutriation rate proportional to total air flow, and (9) overbed combustion rate proportional to air flow and in-bed combustion rate. Assumptions 1, 2 and 3 have been used in modeling conventional steam generators [7–10]. Assumptions (4–9), which will be discussed more fully in this section, are unique to the fluidized-bed system and reflect areas of current research into heat transfer coefficients, flue gas residence time, bed depth, etc. In the model reported here, simple relations or constant input values

Nomenclature

A = area
C = specific heat
F = fluid flow rate
H = fuel heating value, effective
h = specific enthalpy
K = constant
k = thermal conductivity of tube material
ℓ = length
M = flow rate of solid materials
m = mass
p = fluid pressure
Q = heat transfer rate
r = tube radius
T = temperature
t = time
u = specific internal energy
V = volume
α = part of Q_b* due to conduction and convection
β = part of M_f consumed in bed
η = exponent for convection heat transfer coefficient
Θ = conversion factor to absolute temperature
ρ = density
τ = time-constant related to fuel residence time

Superscript

* = design condition

Subscripts

a = average
b, bg, bz = bed, gaseous products in bed, solid materials in bed
$b\ell$ = boiling
c = convection tube water
d = air damper
e = elutriated material
f, fx = fuel, fraction consumed in bed
fd = forced draft fan
fg = flue gas
fw = feedwater
h = freeboard
i = inlet, inner
id = induced draft fan
j = door coolant
ℓ = limestone
m, mi, mo = tube material, inner surface, outer surface
o = outlet, outer
ob = overbed combustion
pa, pg = air at constant pressure, gas at constant pressure
q = carrier air
s = saturated steam
sv = steam valve
t = fluidized air
u = dumped materials from bed
vg = gas at constant volume
w = saturated water

have been assumed for certain variables and parameters. The model structure permits them to be readily changed or replaced when more appropriate information is available.

In utilizing the model, it is assumed that for the particular coal and limestone being utilized, and for their respective particle size distributions, coal residence time and elutriation rate, for example, will be calculated initially and used as model input parameters. The purpose of the model is not to determine such parameters which pertain primarily to processes occurring within the bed itself, but rather to study their effect on the overall steam generator system.

Model equations are developed in the following subsections and rationale for selection of state variables is discussed. Input and state variables are listed in the Appendix.

Fluidized-Bed. The control volume selected for modeling fluidized-bed dynamics is shown in Fig. 3. Its top surface determines bed depth which is a function of time-dependent process variables such as superficial velocity, mass of solid materials, etc. No explicit functional relations for bed depth appear to be available in the literature. Since bed depth is customarily held constant during individual experiments, heat transfer areas, bed mass, etc., are computed assuming constant bed depth for each experimental condition. Thus, fixed control volume is assumed. A time-varying control volume [10] can be incorporated in the model when a suitable analytical relation for bed depth is available.

Mass conservation in the control volume yields

$$\frac{d}{dt}(m_{bg} + m_{bz}) = M_f + M_\ell + F_t + F_q - F_{bg} - M_e - M_u \quad (1)$$

Air and flue gas dynamics inside the cell were found to be very fast, with time constants less than a few milliseconds. Control systems and measuring instruments are low pass filters with respect to such transients, which will have little bearing on overall process dynamics and controller design. Thus, dm_{bg}/dt is set to zero and flue gas flow is computed algebraically by direct mass balance with air flow and instantaneous rate of coal combustion. This is equivalent to setting one eigenvalue of the linearized system to negative infinity.

$$F_{bg} = F_t + F_q + M_{fx} \quad (2)$$

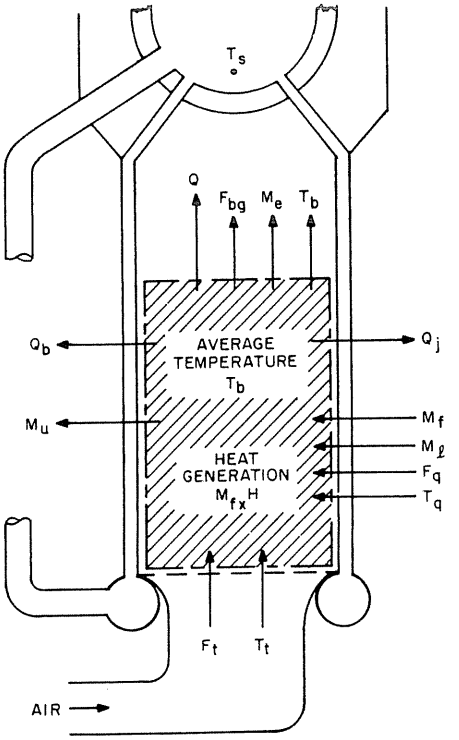

Fig. 3 Fluidized-bed control volume

The sulfur fraction in coal adds to bed mass by the sulfation reaction. CO_2 evolution by calcination of freshly added limestone reduces bed mass. For a Ca:S mol ratio of two, the gain and loss in bed mass approximately balance, and these effects are ignored in the model.

Mass flow of elutriated solids is assumed proportional to total air flow. The proportionality constant is characteristic of the coal and bed material being used.

$$M_u = K_u(F_t + F_q) \quad (3)$$

Coal combustion dynamics inside the bed are approximated by a first order lag.

$$M_{fx} = \frac{m_f}{\tau}; \quad \frac{dM_{fx}}{dt} = \frac{1}{\tau}\frac{dm_f}{dt} = \frac{1}{\tau}(\beta M_f - M_{fx}) \quad (4)$$

Coal introduced into the burning bed has a volatile component which burns in a few seconds, and a solid char component which burns slowly [11]; mass fractions for each component are often comparable. In equation (4), τ is related to an average residence time assumed to be characteristic of the coal being burned, including its char reaction rate and fractional partition into volatile and solid components. Although an Arrhenius temperature dependence of char reaction rate could be included in τ, the simplifying assumption of temperature independence has been made for the following reasons: (1) rapid combustion of the volatile component diminishes the effect of char combustion rate temperature dependence; (2) in normal operation, during which stable combustion is assumed, the range of bed temperature variation will be kept small (perhaps ± 60°C); and (3) in terms of overall steam generator performance, thermal relaxation time of stored energy in the bed (a very slow process) has a much greater effect on system response than changes in char combustion rate.

In this paper, a constant value of $\tau = 10$ s has been assumed. A more detailed functional relationship can be incorporated in the model when available. Similarly, β, the coal fraction consumed in the bed, is assumed to be a constant characteristic of the coal type and bed material; it can also be replaced by some other functional relationship if necessary. System senstivity to τ and β can be readily investigated with the model.

Substituting equation (2) in (1) and setting $dm_{bg}/dt = 0$,

$$\frac{dm_{bz}}{dt} = M_f + M_\ell - M_{fx} - M_e - M_u \quad (5)$$

Equation (5) represents solid mass dynamics in the bed, which behave as a free integrator in the absence of a bed level controller. An ideal bed level controller was assumed which brings bed mass to steady-state value instantaneously, and

$$\frac{dm_{bz}}{dt} = 0; \quad M_u = M_f + M_\ell - M_{fx} - M_e \quad (6)$$

The effect of an ideal controller is to eliminate one eigenvalue of the linearized system. (This is analogous to drum water level control which is discussed in a later section). Without an ideal controller, it is necessary to postulate or simulate a real controller whose characteristics could influence mass storage dynamics in the fluidized-bed.

Average bed temperature, selected as a state variable, provides dynamic information about fluidized-bed thermal conditions. The governing equation is obtained from dynamic energy balance for gases and solids in the control volume (see Fig. 3). Assuming $dm_{bg}/dt = 0$ as discussed previously, and ideal bed level control $dm_{bz}/dt = 0$,

$$\frac{dT_b}{dt} = [(M_f C_f + M_\ell C_\ell)T_q - (M_e + M_u)C_{bz}T_b + (F_t T_t + F_q T_q)C_{pa} - F_{bg}T_b C_{pg} + M_{fx}H - \Sigma Q_b]/(m_{bz}C_{bz} + m_{bg}C_{vg}) \quad (7)$$

ΣQ_b is total heat transfer rate from bed, and thermal energy generated in the bed is $M_{fx}H$ which is the product of effective coal heating value and instantaneous combustion rate.

Mass of gas in the bed is obtained as

$$m_{bg} = (V_b - m_{bz}/\rho_{bz})\rho_{bg} \tag{8}$$

where ρ_{bg} is the average gas density. Since $m_{bg} \ll m_{bz}$ and m_{bg} occurs only in equation (7) in conjunction with m_{bz}, approximating ρ_{bg} by a constant average value improves computational efficiency. However, ρ_{bg} can be evaluated assuming isobaric conditions ($\rho_{bg}(T_b + \Theta)$ = constant), which is justified because variations in absolute bed pressure are small.

Main Air Flow. Main air flow is damper-regulated, and is computed from pressure drop across ducts, damper and distributor plate. Typically, fluid flow F is expressed in terms of inlet and exit pressures, and average density [12].

$$F \propto \sqrt{(p_i - p_o)\rho_a} \tag{9}$$

Assuming constant spatial temperature distribution, average density is approximately proportional to average pressure $\rho_a = (p_i + p_o)/2$. Therefore,

$$F \propto \sqrt{(p_i^2 - p_o^2)} \tag{10}$$

This approximation yields a simple algebraic expression for main air flow in terms of forced draft fan pressure, bed pressure (above the distributor plate) and damper area; flow resistances due to ducts, damper and distributor plate are lumped together.

$$F_t = \frac{K_d A_d K_{fd}}{\sqrt{(K_d A_d)^2 + K_{fd}^2}} \sqrt{(p_{fd}^2 - p_b^2)} \tag{11}$$

K_d and K_{fd} are calculated from design data.

Similarly, total flue gas flow is obtained in terms of bed pressure and induced draft fan inlet pressure.

$$F_{fg} = K_{fg} \sqrt{(p_b^2 - p_{id}^2)} \tag{12}$$

Total flue gas flow includes gas leaving the bed plus the rate of overbed combustion in the freeboard.

$$F_{fg} = F_{bg} + M_{ob} \tag{13}$$

Overbed combustion rate is assumed proportional to elutriation rate and to coal combustion rate in the bed.

$$M_{ob} = K_{ob}(F_t + F_q)M_{fx} \tag{14}$$

K_{ob} is estimated from system design data.

Equations (2) and (11–14) are combined into a quadratic for F_{fg}, eliminating F_{bg} and p_b.

Heat Transfer. The heat transfer coefficient for immersed waterwall tubes is assumed independent of superficial air velocity, but dependent on bed temperature. Thus, heat transfer rate has a linear part due to conduction and convection, and a nonlinear part due to radiation.

$$Q_b = K_b \ell \left[\alpha + (1 - \alpha) \left(\frac{T_b + T_{mo} + 2\Theta}{T_b^* + T_{mo}^* + 2\Theta} \right) \times \left(\frac{(T_b + \Theta)^2 + (T_{mo} + \Theta)^2}{(T_b^* + \Theta)^2 + (T_{mo}^* + \Theta)^2} \right) \right] (T_b - T_{mo}) \tag{15}$$

α is the fraction of total heat transfer due to conduction and convection at the design load condition, only, for which $T_b = T_b^*$ and $T_{mo} = T_{mo}^*$. K_b and α were evaluated from steady-state experimental data at two different operating conditions.

Boiling heat transfer from waterwall inner surface to water/steam mixture is obtained using the empirical correlation of Thom, et al. [14].

$$Q_{b\ell} = K_b A_i \ell \, exp\,(p_s)(T_{mi} - T_s)^2 \tag{16}$$

Conductive heat transfer through the waterwalls is assumed radial.

$$Q_{b\ell} = \frac{A_i \ell k}{r_i \ln(r_o/r_i)} (T_{mo} - T_{mi}) \tag{17}$$

Equations (16) and (17) are solved simultaneously for $Q_{b\ell}$ eliminating T_{mi}.

Convective heat transfer rates in the freeboard, convection tube bank, air preheater, etc., are computed using established formulae [13, 14]. Heat transfer coefficients are assumed flow-dependent, only.

$$Q \propto AF^{\eta}\Delta T \tag{18}$$

The proportionality constant is determined from fluid properties at mean thermodynamic conditions.

Door Coolant. A small part of the energy generated in the bed is absorbed by the water-cooled access door.

$$Q_j = F_j(T_{jo} - T_{ji}) \tag{19}$$

(Specific heat of cooling water is taken to be unity). Because of constant flow, bed to cooling water heat transfer is approximately

$$Q_j = K_j(T_b - T_{ja}) \tag{20}$$

K_j includes heat transfer area and coefficient. Mean water temperature is obtained as a weighted average of inlet and outlet water temperatures.

$$T_{ja} = T_{ji} + (1 - \xi)T_{jo}, \qquad 0 < \xi < 1 \tag{21}$$

Equations (19–21) are solved for Q_j and T_{jo} in terms of input variables F_j and T_{ji}.

Freeboard. The steam drum is located in the freeboard directly above the fluidized bed. Transients associated with freeboard stored energy are very high frequency, and energy balance for freeboard gases and solids is considered in steady-state form.

$$Q_h = M_{ob}H + (F_{fg}C_{pg} + M_eC_{bz})(T_b - T_{ho}) - M_{ob}(C_{pg}T_b - C_{bz}T_{ho}) \tag{22}$$

Using equation (18) for convective heat transfer from freeboard to waterwalls, and treating mean freeboard temperature as a weighted average of T_b and T_{ho} (as in equation 21), the resulting equations are solved simultaneously for Q_h and T_{ho}.

Radiative heat transfer above the bed, expressed in the form

$$Q \propto [(T_b + \Theta)^4 - (T_{mo} + \Theta)^4] \tag{23}$$

is applied separately to freeboard waterwalls and drum surface. The proportionality constants include emissivity, effective surface area, and the Stefan-Boltzmann constant.

Convection Tube Bank. After flowing past the drum, flue gas is cooled by convection tubes where a substantial amount of energy is absorbed. Flue gas temperature entering this section is obtained by direct heat balance. Temperature drop across thin tube walls is neglected. Heat transfer Q_c from flue gas to convection tube water is obtained by combining heat transfer coefficients from flue gas to tube wall and from tube wall to water.

Treating water as incompressible, conservation of energy in the tube water control volume yields

$$\frac{d}{dt} T_{ca} = [F_c(T_{ci} - T_{co}) + Q_c]/m_c \tag{24}$$

Outlet water temperature T_{co} is extrapolated from inlet and average temperatures, T_{ci} and T_{ca}, as in equation (21).

Drum and Waterwall Tubes. The drum model is formulated using established techniques [8], assuming saturated conditions and uniform pressure. Mass and energy conservation in the drum control volume yield

$$\frac{d}{dt}(\rho_s V_s + \rho_w V_w) = F_{fw} - F_s \tag{25}$$

$$\frac{d}{dt}(\rho_s V_s u_s + \rho_w V_w u_w) = F_{fw}h_{fw} - F_s h_s + \Sigma Q_{b\ell} \tag{26}$$

$\Sigma Q_{b\ell}$ is total heat transfer rate to water/steam. ρ_s and V_w are selected as state variables, and thermodynamic properties of water and steam at saturated conditions are expressed as functions of ρ_s. Using partial derivatives of thermodynamic variables with respect to ρ_s, equations (25) and (26) become

$$\left(V_s + V_w \frac{\partial \rho_w}{\partial \rho_s}\right) \frac{d\rho_s}{dt} + (\rho_w - \rho_s) \frac{dV_w}{dt} = F_{fw} - F_s \quad (27)$$

$$\left[V_s \left(u_s + \frac{\partial u_s}{\partial \rho_s} \rho_s\right) + V_w \left(u_w \frac{\partial \rho_w}{\partial \rho_s} + \rho_w \frac{\partial u_w}{\partial \rho_s}\right)\right] \frac{d\rho_s}{dt}$$
$$+ (\rho_w u_w - \rho_s u_s) \frac{dV_w}{dt} = F_{fw} h_{fw} - F_s h_s + \Sigma Q_{b\ell} \quad (28)$$

which are solved algebraically for $d\rho_s/dt$ and dV_w/dt.

Saturated steam flow vented to the atmosphere is determined from drum pressure assuming choked flow in the steam flow control valve [12].

$$F_s = K_{sv} A_{sv} \sqrt{p_s \rho_s} \quad (29)$$

Feedwater flow F_{fw}, determined by pressure drop across the flow control valve, is regulated by a controller whose response is fast with respect to drum level transients. During experimental runs, drum level hardly changes. Consequently, an ideal drum level controller is assumed, with feedwater and steam flow rates balanced at every instant. dV_w/dt is set to zero, and drum level is constant.

Thermal energy stored in waterwall tube metal, as well as in the water/steam mixture inside the tubes, and heat transfer from tube metal to the water/steam mixture are considered separately for the bed and the freeboard regions because of different thermal dynamics using the form of equations (16) and (17). Heat transfer areas and thermal capacitances of these regions are directly proportional to their respective lengths, and average outer tube wall surface temperatures are selected as state variables. Since waterwall steam quality varies with firing rate, lumped average thermal capacitance changes with load. However, fixed average values were assumed for bed and freeboard regions because thermal capacitance of tube material is significantly larger than that of water.

Gas Emission Characteristics. In a fluidized-bed steam generator, limestone feed rate is controlled on the basis of SO_2 concentration; air flow and coal feed rate are influenced by O_2 concentration. Thus, O_2 and SO_2 concentrations must be available as output variables when the model is applied to analytical controller design. An understanding of fluidized-bed chemical kinetics, a subject of current research, is required to formulate model equations for O_2 and SO_2 concentration, and is not included in this paper.

Experimental Program and Model Validation

A flexible data acquisition system ideally suited to recording data during transient response tests, as well as steady-state operation, has been installed at the Alexandria Process Development Unit. Signals from up to 128 channels can be sampled, amplified, digitized, and stored on magnetic tape. Scanning of all 128 channels can be repeated as often as five times per second. Normally, the period between scans is 1–4 s.

For the measurements reported here, the scan list consists of 18 flow rate, 14 pressure, one level, 35 temperature, and eight gas analysis signals, plus a variety of test and calibration signals. Characteristics of the data acquisition system have been described elsewhere [15]. Copies of magnetic tapes are available for studying the process in more detail.

Major input variables manipulated for open loop transient response tests are: (1) rotary coal feeder speed to change firing rate, (2) inlet air damper position to change fluidizing air flow, and (3) drum steam valve position to change steam pressure and steam flow rate. Feedwater valve operation is normally on automatic control to insure stable drum water level; it was not available for changing feedwater flow.

Initial tests were conducted to obtain steady-state data at several operating conditions corresponding to different firing rates and bed depths. Observed steady-state values were compared with predicted values of process variables for validating the model as an acceptable steady-state process description.

The area of greatest model uncertainty concerns the heat transfer coefficient for immersed surface. Parameters and equation structure in that portion of the model were adjusted to obtain close agreement between model predictions and measured performance at several operating points. This adjustment provided deeper insight into process characteristics, requiring detailed examination of modeling assumptions and equation structures and adoption of the temperature dependence expressed in equation (15).

Transient response tests involved independent step changes in rotary coal feeder speed and inlet air damper position. To achieve agreement between model transient response predictions and observed data depicted in the figures which follow, it was necessary to increase thermal capacity of the fluidized-bed approximately 20 percent. This reflects the fact that the limestone bed partially converts to calcium sulfate with a higher density and specific heat, which was not considered in the initial estimate of bed thermal capacity.

Model Results

Comparisons of steady-state model predictions and test results at two different load levels are given in Table 1. These two operating conditions were starting points for transient response tests. Figs. 4–6 compare transient response predictions with measured values of bed temperature, drum steam pressure, and steam flow, respectively, for an 8.22 percent step decrease in coal feed rate. Equivalent static bed depth for this test was 0.508 m (20 in.). Model results for bed temperature transients (Fig. 4) agree closely with experimental data. For drum steam pressure (Fig. 5), model predictions appear somewhat faster than test data. This may be due to inaccuracy in drum water level, i.e., drum water thermal capacitance. Steam flow data (Fig. 6) is noisy, due to instrumentation, but the average profile appears to agree with model results.

Table 2 shows system eigenvalues of the linearized model at steady-state conditions before and after the 8.22 percent decrease in coal feed rate. The eigenvalues decrease at lower firing rate, indicating that the process slows down. The smallest eigenvalue is strongly associated with fluidized-bed thermal relaxation and corresponds to a time-constant of approximately 220 s before the change and 235 s after, which illustrates the effect of process nonlinearity. The −0.100 eigenvalue corresponds to coal residence time constant in the bed during combustion, which is assumed to have a constant value of 10 s.

Figs. 7–9 compare model transient response with measured values of bed temperature, drum steam pressure, and steam flow for a 6.75 percent increase in main air flow. Equivalent static bed depth for this test was 0.305 m (12 in.). For bed temperature (Fig. 7), model results and test data are in close agreement until about ten minutes after the disturbance, when test results show an upward drift. This was caused by a small inadvertent increase in coal feed rate which was identified by a decrease in observed flue gas O_2 content. This drift is also obvious in drum steam pressure response (Fig. 8) but cannot be identified in the noisy steam flow response (Fig. 9).

Following the air flow disturbance, both model results and test data show an initial overshoot in steam pressure (Fig. 8) which then relaxes to a lower value. Overshoot occurs in response to increasing flue gas flow and convective heat transfer in the freeboard. Then, as bed temperature decreases, flue gas temperature drops reducing freeboard heat transfer below the initial level. Test data show a larger overshoot than model results attributed to inaccuracy in formulating model equations for overbed combustion, which for the model reported here, probably underestimated the portion of total heat transfer to drum and waterwalls in the freeboard region.

Conclusions

A dynamic model of an atmospheric pressure fluidized-bed combustion steam generation system has been developed, and model results verified with experimental data for both steady-state and transient performance. The state-space model structure allows digital simulation and analytical controller design. Furthermore, the model can be used for design verification and predicting effects of subsystem changes on the entire process.

Simple correlations for fluidized-bed heat transfer coefficient and fuel residence time were assumed due to lack of more reliable data. However, the model structure allows replacement and addition of appropriate functional relationships without difficulty. Even in the present form, the model closely represents the actual process and has

Table 1 Comparison of steady-state model results with test data

Process Variables	*Model Results*	*Test Data*
	Bed depth 0.508 m (20 in.)	
Bed Temperature	884.4°C (1624°F)	882.2°C (1620°F)
Drum steam pressure	0.7633×10^6 N/m^2 (110.7 psia)	0.7653×10^6 N/m^2 (111 psia)
Main steam flow	0.3404 kg/s (0.7504 lbm/s)	0.3402 kg/s (0.75 lbm/s)
Coal feed rate*	0.0857 kg/s (0.189 lbm/s)	0.0857 kg/s (0.189 lbm/s)
Limestone feed rate*	0.0367 kg/s (0.0809 lbm/s)	0.0367 kg/s (0.0809 lbm/s)
FD Fan air flow	0.5770 kg/s (1.272 lbm/s)	0.5783 kg/s (1.275 lbm/s)
Carrier air flow*	0.0506 kg/s (0.1114 lbm/s)	0.0506 kg/s (0.1114 lbm/s)
	Bed depth 0.304 m (12 in.)	
Process Variables	*Model Results*	*Test Data*
Bed Temperature	920.56°C (1689°F)	918.33°C (1685°F)
Drum steam pressure	0.7543×10^6 N/m^2 (109.4 psia)	0.7584 N/m^2 (110 psia)
Main steam flow	0.3329 kg/s (0.7339 lbm/s)	0.3311 kg/s (0.73 lbm/s)
Coal feed rate*	0.0844 kg/s (0.186 lb/s)	0.0844 kg/s (0.186 lbm/s)
Limestone feed rate*	0.0367 kg/s (0.0809 lbm/s)	0.0367 kg/s (0.0809 lbm/s)
FD Fan air Flow	0.516 kg/s (1.238 lbm/s)	0.5171 kg/s (1.240 lbm/s)
Carrier air flow*	0.0506 kg/s (0.1114 lbm/s)	0.0506 kg/s (0.1114 lbm/s)

* Given as input to the model

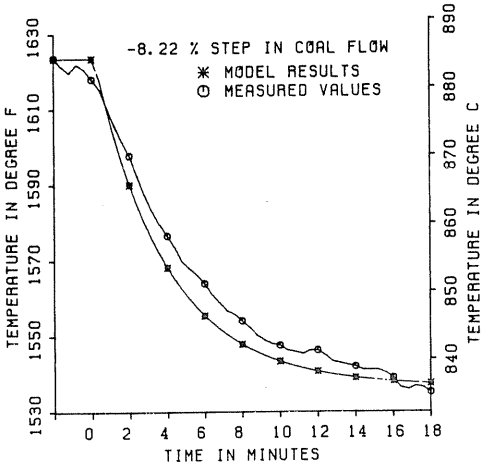

Fig. 4 Bed temperature transient due to 8.22 percent step decrease in coal feed rate

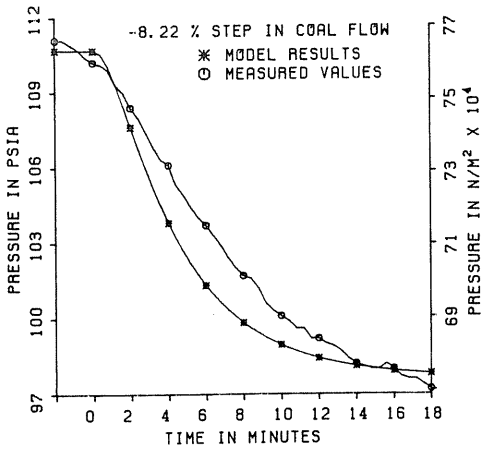

Fig. 5 Drum steam pressure transient due to 8.22 percent step decrease in coal feed rate

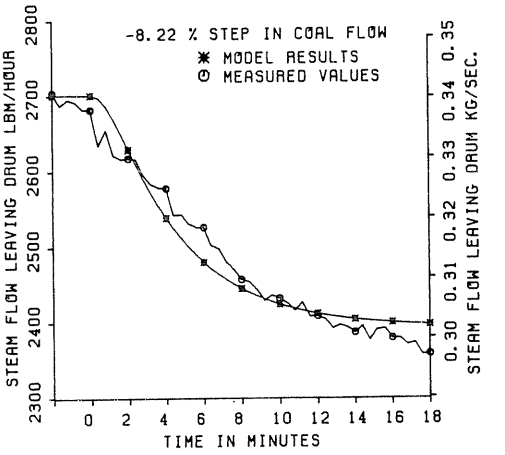

Fig. 6 Steam flow transient due to 8.22 percent step decrease in coal feed rate

Table 2 Eigenvalues of linearized model before and after −8.22 percent change in coal feed rate

Before	*After*
$-.00451\ s^{-1}$	$-.00425\ s^{-1}$
−.00642	−.00641
−.0103	−.0103
−.0168	−.0162
−.100	−.100
−.535	−.524
−.780	−.764

become a useful tool in studying the less well-understood parts of it.

Although the model is related to a particular fluidized-bed plant, the method of analysis has general applicability and can be readily adapted to study other fluidized-bed steam power generation systems.

Acknowledgment

This work was supported by the Coal Conversion and Utilization Division of ERDA/Fossil Energy under Contract Number EX-76-C01-2453. The experimental facility at Alexandria, Va., is operated for ERDA by Pope, Evans and Robbins. The authors are thankful to Mr. Mark D. Wilson for assistance in formulating the model.

References

1 Kunii, D. and Levenspiel, O., *Fluidization Engineering*, Wiley, New York, 1969.

2 Berkowitz, D. A., Ray, A., Sumaria V. and Wilson, M. D., "Dynamic Modeling Testing and Control of Fluidized Bed Systems," *Proceedings of 5th International Conference on Fluidized Bed Combustion*, Dec. 12–14, 1977, Washington, DC.

3 Lin, Y., Nielsen, R. S., and Ray, A., "Fuel Controller Design in a Once-through Subcritical Steam Generator System," ASME JOURNAL OF ENGINEERING FOR POWER, Vol. 100, No. 1, Jan. 1978, pp. 189–196.

4 Berkowitz, D. A., ed., *Proceedings of the Seminar on Boiler Modeling*, The MITRE Corporation, Bedford, MA., Oct. 1975.

5 *IBM Continuous System Modeling Program (CSMP-III)*, Program Reference Manual Ser. No. SH19-7001-2, Sept. 1972.

6 Springer, T. E. and Farmer, O. A., "TAF—A Steady State, Frequency Response Simulation Program," *Proceedings-Fall Joint Computer Conference*, 1968.

7 Adams, J., Clark, D. R., Louis, J. R., and Spanbauer, J. P., "Mathematical Modeling of Once-through Boiler Dynamics," *IEEE Trans.*, PAS-84, Feb. 1965,

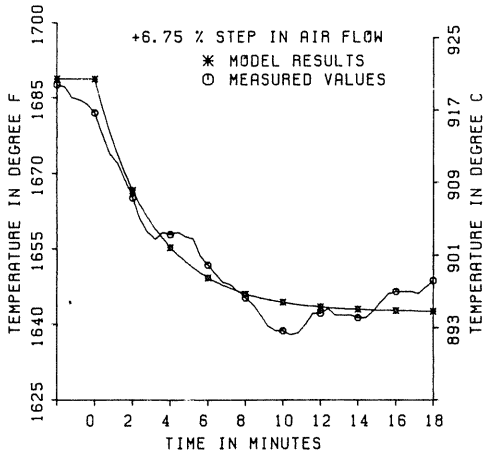

Fig. 7 Bed temperature transient due to 6.75 percent step increase in air flow

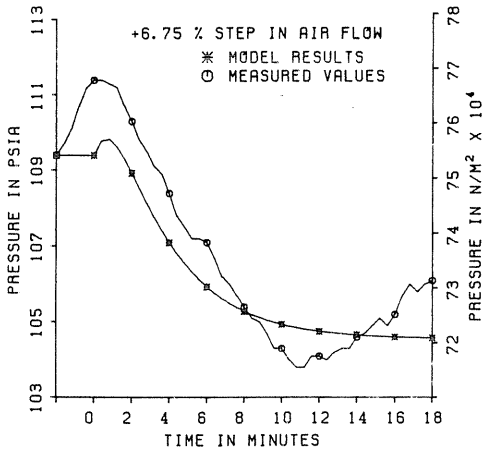

Fig. 8 Drum steam pressure transient due to 6.75 percent step increase in air flow

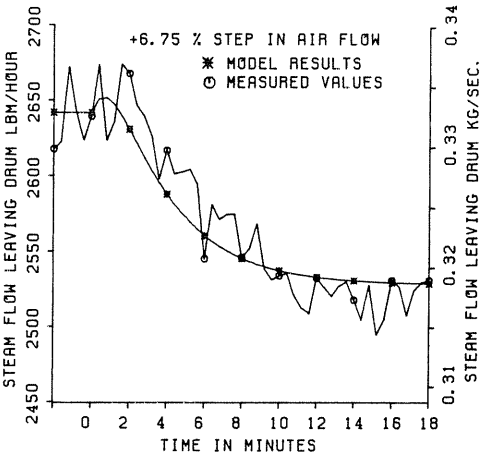

Fig. 9 Steam flow transient due to 6.75 percent step increase in air flow

pp. 146–156.

8 Kwatny, H. G., McDonald, J. P., and Spare, J. H., "A Nonlinear Model for Reheat Boiler-Turbine-Generator Systems: Part II-Development," *Proceedings of Joint Automatic Control Conference*, 1971, pp. 227–236.

9 McNamara, R. W., Ringham, M. R., Bramblett, C. C. and Southworth, L. C. "Practical Simulation of an Industrial Fluid System with Controls—The Circulator Auxiliaries for the Fort St. Vrain Nuclear Generating Station," *Proceedings of Joint Automatic Control Conference*, 1977, pp. 332–339.

10 Ray, A. and Bowman, H. F., "A Nonlinear Dynamic Model of a Once-through Steam Generator," ASME *Journal of Dynamic Systems, Measurement and Control*, Vol. 98, No. 3, Sept. 1976.

11 Beer, J. M., Baron, R. E., Borghi, G., Hodges, J. L. and Sarofim, A. F., "A Model of Coal Combustion in Fluidized Bed Combustors," *Proceedings of 5th International Conference on Fluidized Bed Combustion*, Dec. 12–14 1977, Washington, DC.

12 Blackburn, J. F., Reethof, G., and Shearer, L., eds., *Fluid Power Control*, M.I.T., Cambridge, 1960.

13 Rohsenow, W. M., and Hartnelt, J. P., eds., *Handbook of Heat Transfer*, McGraw-Hill, New York, 1973.

14 Holman, J. P., *Heat Transfer*, McGraw-Hill, 1976

15 Berkowitz, D. A., Ray, A., and Sumaria, V., "Dynamic Modeling of Fluidized-Bed Boilers for Control System Design," *Proceedings of 12th International Energy Conversion Engineering Conference*, Aug. 28–Sept 2, 1977, Washington, D. C.

APPENDIX

List of Model Input Variables and State Variables

The model input variables and state variables, together with steady-state values at a typical operating condition, are listed below:

Input Variables

u_1 coal feed rate 0.0837 kg/s (0.1846 lbm/s)

u_2 main air flow damper area (normalized) 0.85

u_3 drum steam flow valve area (normalized) 0.8

u_4 limestone feed rate 0.03674 kg/s (0.081 lbm/s)

State Variables

x_1 average bed temperature 884.22°C (1623.6°F)

x_2 instantaneous coal combustion rate in the bed 0.0728 kg/s (0.1605 lbm/s)

x_3 average waterwall outer surface temperature in the immersed region 194.22°C (381.6°F)

x_4 average waterwall outer surface temperature in the freeboard region 178.44°C (353.2°F)

x_5 average cooling water temperature in the convection tube bank 50.54°C (122.98°F)

x_6 average tube wall temperature at the mean radius in air preheater 309.39°C (588.9°F)

x_7 saturated steam density in the boiler drum 3.992 kg/m^3 (0.2492 lbm/ft^3)

x_8 drum water volume 0.30667 m^3 (10.83 ft^3)

x_9 mass of solid materials in the bed 725.75 kg (1600 lbm)

The state variables x_8 and x_9 are held fixed at constant values, and $\dot{x}_8$ and $\dot{x}_9$ are constrained to zero.